World Academy of Science, Engineering and Technology
International Journal of Mechanical and Mechatronics Engineering
Vol:9, No:6, 2015

Disturbance Observer for Lateral Trajectory Tracking Control for Autonomous and Cooperative Driving

Christian Rathgeber, Franz Winkler, Dirk Odenthal, Steffen Müller

***Abstract*—**In this contribution a structure for high level lateral vehicle tracking control based on the disturbance observer is presented. The structure is characterized by stationary compensating side forces disturbances and guaranteeing a cooperative behavior at the same time. Driver inputs are not compensated by the disturbance observer. Moreover the structure is especially useful as it robustly stabilizes the vehicle. Therefore the parameters are selected using the Parameter Space Approach. The implemented algorithms are tested in real world scenarios.

***Keywords*—**Disturbance observer, trajectory tracking, robust control, autonomous driving, cooperative driving.

I. Introduction

IN the last century advanced driver assistance systems (ADAS) have prevailed more and more in the vehicle. Initially it was mainly longitudinal guidance systems or parking systems. More recently, lateral vehicle guidance systems using electronic power steering have been introduced into market. Thereby functions like lanekeeping assistance can be implemented. With such functions the driver assistance system and the driver handle the task of driving together (cooperative driving). In the future, functions are also possible in which the ADAS will completely take over the lateral guidance.

The aim of this paper is therefore to introduce a control structure for high-level lateral control that can handle both cooperative maneuvers in interaction with the driver as well as hands off maneuvers.

Since the control structure is to be applied in a wide variety of vehicles in different operating conditions (i.e. varying mass), methods of robust control are considered. In the robust control theory the so-called disturbance observer [1] has proven. It is used in a large number of applications and provides robust and stationary accurate control results. As will be shown, the disturbance observer is particularly useful for the task of cooperative driving. A modification of the usual disturbance observer structure allows to compensate only a part of the disturbances and thus not compensating the driver input.

Christian Rathgeber is with BMW AG, 80937 Munich, Germany (e-mail: christian.rathgeber@bmw.de)
Franz Winkler is with BMW AG, 80937 Munich, Germany (e-mail: franz.winkler@bmw.de)
Dirk Odenthal is with BMW AG, 80937 Munich, Germany (e-mail: dirk.odenthal@bmw.de)
Steffen Müller is with Technical University of Berlin, 13355 Berlin, Germany (e-mail: steffen.mueller@tu-berlin.de)

Concerning lateral control a lot of contributions have dealt with the topic. Most of them concentrate on autonomous driving, i.e. without driver interaction. It exist for example approaches based on linear controller design [2], nonlinear controller design [3] or modelpredictive control [4].

This contribution is organized as follows: Section II gives a brief overview of the control structure. In Section III, we recall the kinematic system dynamics of the vehicle relative to a road and a planned trajectory. The control design will be based on this model. In Section IV the theory of the disturbance observer is briefly summarized and a variation of the usual structure is presented. Based on this, the control design is presented in Section V. Section VI outlines the advantages of the presented control structure for cooperative driving and in Section VII the tuning of the control parameters is explained using the Parameter Space Approach. The presented control structure is finally evaluated in Section VIII in real-world scenarios.

II. Control Structure

The control structure is based on the two-degrees of freedom structure. Thus it is possible to separately define the command response and disturbance attenuation. Fig. 1 shows the structure. The trajectory planning and feedforward

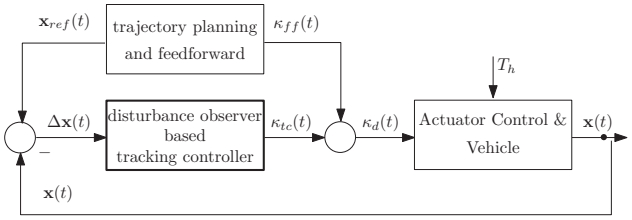

Fig. 1: Control structure

control calculate the feedforward signal κ_{ff}. It also provides the reference signals $\mathbf{x}_{ref}$ for the controller. The controller suppresses deviations $\Delta\mathbf{x}$ caused by disturbances and model deviations with the control signal κ_{tc}. A usual controller with integrating behavior would also compensate the driver inputs T_h. To introduce a controller showing a cooperative behavior concerning the driver input is the aim of this contribution.

III. Modeling

For modeling the lateral dynamic behavior of the vehicle the well-known single-track model is used [5]. The yaw rate

$\dot{\psi}$ and the slip angle β represent the state variables. They result from the transfer functions

$$\dot{\psi} = G_{\dot{\psi}}(s)\,\delta \tag{1}$$

and

$$\beta = G_{\beta}(s)\,\delta \tag{2}$$

with δ being the steering angle, representing the input. The derivation of the equations is described in the Appendix. Since the transient behavior of the tire forces is taken into account both transfer functions have PD_2T_4 behavior (i.e. relative degree 2).

The steering angle is controlled by a lower-level control like presented in [6]. For the sake of simplicity it is assumed that the dynamic behavior of the steering and its controller can be represented by a PT_2-behavior. Thereby, not the desired steering angle is used as an input but the desired curvature κ_d. Thus, δ results as

$$\delta = G_{\delta}(s)\,\kappa_d = \frac{K_{\delta}}{\tau_{\delta}^2 s^2 + 2D_{\delta}\tau_{\delta} + 1}\,\kappa_d. \tag{3}$$

τ_{δ} and D_{δ} describe the time constant and damping. The unity gain K_{δ} can be calculated as

$$K_{\delta} = l\left(1 + \left(\frac{v}{v_{ch}}\right)^2\right) \tag{4}$$

where l is the vehicle wheelbase, v_{ch} the characteristic velocity and the v the longitudinal velocity.

To describe the vehicle movement relative to the road and a planned trajectory the heading angle ψ_r is used (see Fig. 2). It describes the differential angle between the vehicle

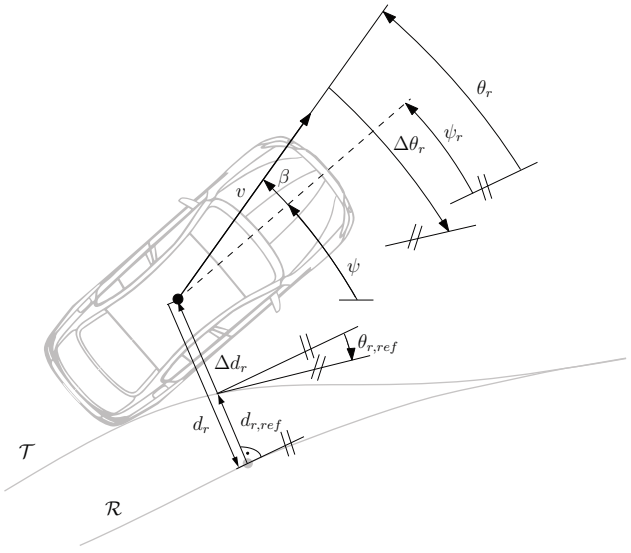

Fig. 2: Vehicle relative to the road and a planned trajectory

longitudinal axis and the tangent to the road $\mathcal{R}$ and results from

$$\dot{\psi}_r = \dot{\psi} - v\,\kappa_s. \tag{5}$$

κ_s is the road curvature. For the control the so-called course angle θ_r is required. It is obtained by considering the slip angle

$$\theta_r = \psi_r + \beta. \tag{6}$$

Furthermore, the lateral deviation is required, describing the shortest distance to the road. Its differential equation is

$$\dot{d}_r = v\,\theta_r. \tag{7}$$

The used trajectory planning calculates a trajectory $\mathcal{T}$ relative to the road $\mathcal{R}$. It is described by the reference curvature $\kappa_{r,ref}$, the reference course angle $\theta_{r,ref}$ and the reference lateral deviation $d_{r,ref}$. Hence the control errors result as

$$\Delta\theta = \theta_{r,ref} - \theta_r \tag{8}$$

and

$$\Delta d = d_{r,ref} - d_r. \tag{9}$$

The main disturbances that have to be compensated, result from side force disturbances F_{yd} and moment disturbances M_{zd}. They are caused by lateral force disturbances which can for example result from crosswinds or hanging roadways. Both result in a yaw rate disturbance $z_{\dot{\psi}}$ and a slip angle disturbance z_{β}.

IV. Disturbance Observer

The theory of the disturbance observer (DO) was first introduced in [1]. It has been widely employed due to its robust compensation of disturbances and plant uncertainties. For example it has been used for the design of a steering angle controller [7], a control for a DC Servo Motor [8] and the position control of a industrial robot [9]. Usually the disturbance observer provides an estimation $\tilde{z}$ of the disturbance z which is used for compensation. For this purpose the disturbance observer compares the input u and the output y of the plant by inverting a model of the plant $\tilde{G}(s)$. To realize the inversion a filter $Q(s)$ is used. Fig. 3 shows the common structure of the disturbance observer. n denotes measurement noise. The closed loop transfer functions are given by

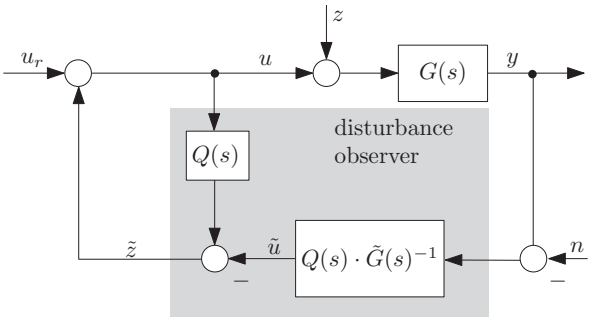

Fig. 3: Structure of the disturbance observer

$$G_{u_r y}(s) := \frac{Y(s)}{U_r(s)} = \frac{G(s)\tilde{G}(s)}{\tilde{G}(s) + (G(s) - \tilde{G}(s))Q(s)}, \tag{10}$$

$$G_{zy}(s) := \frac{Y(s)}{Z(s)} = \frac{G(s)\tilde{G}(s)(1 - Q(s))}{\tilde{G}(s) + (G(s) - \tilde{G}(s))Q(s)}, \tag{11}$$

$$G_{ny}(s) := \frac{Y(s)}{N(s)} = \frac{G(s)Q(s)}{\tilde{G}(s) + (G(s) - \tilde{G}(s))Q(s)}. \tag{12}$$

For low frequencies $(Q(s) \approx 1)$ results:

$$G_{u_r y}(s) \approx \tilde{G}(s), G_{zy}(s) \approx 0, G_{ny}(s) \approx 1 \tag{13}$$

and high frequencies $(Q(s) \approx 0)$:

$$G_{u_r y}(s) \approx G(s), G_{zy}(s) \approx G(s), G_{ny}(s) \approx 0 \tag{14}$$

At low frequencies the DO based control loop behaves like the nominal plant $\tilde{G}(s)$ and at high frequencies like the real plant $G(s)$. That means for low frequencies the structure impresses the nominal behavior of $\tilde{G}(s)$ to the plant. This may facilitate that the control design of the outer controller can be performed for the nominal model $\tilde{G}(s)$. Therefore the transient behavior is the same in the presence of disturbances and parameter uncertainties. This is an important feature in industry where robustness and the same transient behavior for different product units is necessary.

[10] showed that the DO can even handle nonlinear behavior of the plant. The effects of nonlinearities can be canceled by the DO and thus make the system behave like the linear nominal model.

The design of the DO is mainly the task of selecting $\tilde{G}(s)$ and $Q(s)$. [11] presents an almost necessary and sufficient condition for guaranteeing robust stability of closes-loop systems with DO. The relative degree of the nominal model $\tilde{G}(s)$ has to be the same as the real plant's relative degree. If this is taken into account and the filter $Q(s)$ is fast enough, then a robust compensation is guaranteed. This means that unknown parameters or disturbances can be controlled robustly.

Concerning the filter $Q(s)$ the following requirements have to be fulfilled:

- relative degree of $Q(s)$ should be greater or equal to the relative degree of $\tilde{G}(s)$ (causality of $Q/\tilde{G}(s)$)
- disturbance rejection at low frequencies
- measurement noise rejection at high frequencies

A low-pass filter with the required relative degree fulfills these requirements and is usually selected (although in some applications a different filter might be useful, see for example [12]).

In some cases it may be useful to divide the dynamics of the plant and to consider them separately. This allows an estimation of only one part of the disturbances. Fig. 4 shows the structure to compensate z_2. The other disturbance z_1 won't be compensated by the DO. The plant is divided in $G_1(s)$ and $G_2(s)$. For example $G_1(s)$ can represent the actuator. The transfer functions of the closed loop are given as:

$$G_{u_r y} = \frac{G_1 G_2 \tilde{G}_1 \tilde{G}_2}{\tilde{G}_1 \tilde{G}_2 + Q_1 Q_2 (G_1 G_2 - G_1 \tilde{G}_2)}, \tag{15}$$

$$G_{ny} = \frac{G_1 G_2 Q_1 Q_2}{\tilde{G}_1 \tilde{G}_2 + Q_1 Q_2 (G_1 G_2 - G_1 \tilde{G}_2)}, \tag{16}$$

$$G_{z_1 y} = \frac{G_1 G_2 \tilde{G}_1 \tilde{G}_2}{\tilde{G}_1 \tilde{G}_2 + Q_1 Q_2 (G_1 G_2 - G_1 \tilde{G}_2)}, \tag{17}$$

$$G_{z_2 y} = \frac{G_2 \tilde{G}_2 (\tilde{G}_1 - G_1 Q_1 Q_2)}{\tilde{G}_1 \tilde{G}_2 + Q_1 Q_2 (G_1 G_2 - G_1 \tilde{G}_2)}. \tag{18}$$

Using this structure, $\tilde{G}_1(s)$ has to represent $G_1(s)$ as accurately as possible that the approximation $G_1(s) \approx \tilde{G}_1(s)$ holds.

Hence, for low frequencies $(Q_1(s) \approx 1, Q_2(s) \approx 1)$ results

$$G_{u_r y}(s) \approx G_1(s)\tilde{G}_2(s), G_{ny}(s) \approx 1, \tag{19}$$

$$G_{z_1 y}(s) \approx G_1(s)\tilde{G}_2(s), G_{z_2 y}(s) \approx 0 \tag{20}$$

and for high frequencies $(Q_1(s) \approx 0, Q_2(s) \approx 0)$

$$G_{u_r y}(s) \approx G_1(s)G_2(s), G_{ny}(s) \approx 0, \tag{21}$$

$$G_{z_1 y}(s) \approx G_1(s)G_2(s), G_{z_2 y}(s) \approx G_2(s). \tag{22}$$

This means that this structure impresses a nominal model $\tilde{G}_2(s)$ to the plant $G_2(s)$ for low frequencies and suppresses disturbances z_2. However $G_1(s)$ has to be known accurately as the disturbance observer won't match the nominal model $\tilde{G}_1(s)$ to $G_1(s)$. The big advantage however is that z_1 won't be estimated and compensated. This characteristic will be utilized in the following controller design.

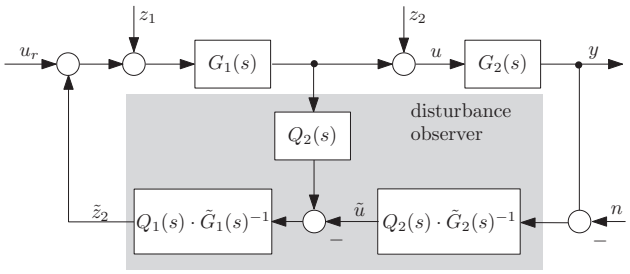

Fig. 4: Modified structure of the disturbance observer to compensate z_2

V. Controller Design

The disturbance observer can be used for the problem of vehicle lateral control. The control structure is based on the considerations of [13]. Fig. 5 depicts the whole control structure. The trajectory planning provides the reference signals $\kappa_{r,ref}$, $\theta_{r,ref}$ and $d_{r,ref}$. A feedforward control calculates the feedforward signal κ_{ff} using a simplified model of the underlying plant. To attenuate disturbances a disturbance observer and a tracking controller are used. Each of them will be explained in the following. The whole control law calculates as

$$\kappa_d = \kappa_{ff} + \kappa_{tc} + \kappa_{do}. \tag{23}$$

As written before the disturbance observer is used to guarantee stationary accuracy. The measured heading angle ψ_r is used as input to the DO. In principle, any signal could be used which lies behind the disturbance that has to be compensated. The main disturbance that has to be eliminated is $z_{\dot{\psi}}$. Therefore $\dot{\psi}$ would be the first choice. However, since the measured road curvature κ_s may differ considerably from the real one, the heading angle ψ_r is used as an input to the DO.

According to the classical implementation of the DO, the

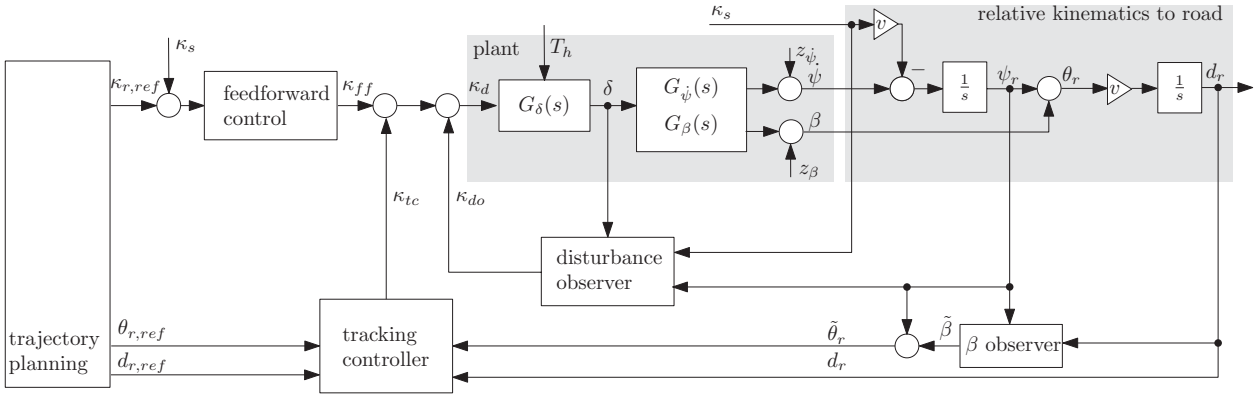

Fig. 5: Proposed control structure for lateral trajectory tracking control

heading angle would be compared to the control output κ_d. It results

$$\kappa_{do} = Q_{do}(s)\left(\kappa_d - \tilde{G}(s)^{-1}\underbrace{\left(\kappa_s + \frac{s}{v}\psi_r\right)}_{\tilde{\kappa}_{\psi_r}}\right). \tag{24}$$

In this case $\tilde{G}(s)$ represents a simplified transfer function of $G_\delta(s) \cdot G_{\dot{\psi}}(s)$. As the heading angle ψ_r is used as an input, the road curvature κ_s has to be considered and ψ_r has to be derived and divided by the vehicle velocity v.
Using the steering angle δ instead of κ_d as an input, the driver intervention is not considered as a disturbance. Therefore δ is transformed to a curvature using (4). The cooperative version of the DO thus calculates as

$$\kappa_{do} = Q_\delta(s)\tilde{G}_\delta(s)^{-1}\,Q_{do}(s)\left(\underbrace{\frac{\delta}{K_\delta}}_{\tilde{\kappa}_\delta} - \tilde{G}(s)^{-1}\underbrace{\left(\kappa_s + \frac{s}{v}\psi_r\right)}_{\tilde{\kappa}_{\psi_r}}\right). \tag{25}$$

In this case $\tilde{G}(s)$ represents the dynamics of $G_{\dot{\psi}}(s)$. Since the real transfer function has relative degree of 2 (see (1)), an ideal damped PT_2 can be used

$$\tilde{G}(s) = \frac{1}{\tau_v^2 s^2 + 2\tau_v s + 1} \tag{26}$$

representing the vehicle nominal dynamics with its time constant τ_v. In contrast to (24), $\tilde{G}_\delta(s)$ has to be considered separately. For its inversion a second filter $Q_\delta(s)$ is necessary. If the underlying steering angle controller is fast enough $\tilde{G}_\delta$ may be neglected.
The benefit of this structure is that driver inputs T_h won't be compensated according to (19) and (20). Thus, it yields

$$G_{T_h \to \kappa_{do}} \approx 0 \tag{27}$$

for the cooperative DO. The underlying steering angle controller also shouldn't compensate the driver's torque that the control behavior is completely cooperative. [6] therefore presents a structure to consider it in the underlying controller. The classical implementation of the DO treats the driver input as a disturbance. Since the DO has integral behavior, the output of the DO would increasingly continue to work against the driver input. This characteristic will be discussed in Section VI in detail.

According to (19) the DO matches the desired behavior to the underlying plant. As mentioned before this feature is useful for the controller design. Varying parameters (e.g. varying mass) can therefore be handled.

The outer loops are based on the feedback of the course angle error and the lateral deviation. The tracking controller law is calculated as

$$\kappa_{tc} = k_\theta \Delta\theta + k_d \Delta d = k_\theta(\theta_{r,ref} - \tilde{\theta}_r) + k_d(d_{r,ref} - d_r). \tag{28}$$

As described in [13], cameras usually don't measure the course angle relative to the road θ_r but the heading angle ψ_r. For a stationary accurate control this is however necessary. Therefore an observer is used to estimate $\tilde{\beta}$. Its transfer function is

$$\tilde{\beta} = Q_\beta(s)\left(\psi_r + \frac{s}{v}d_r\right). \tag{29}$$

Therefore the heading angle and the lateral deviation are used. A filter $Q_\beta(s)$ is necessary to make the differentiation of d_r possible and to guarantee noise cancellation. An ideal damped PT_2 proofed as the best compromise between noise cancellation and fast estimation.
The estimated side slip angle is used to calculate the course angle

$$\tilde{\theta}_r = \psi_r + \tilde{\beta}. \tag{30}$$

For calculating the gains k_θ and k_d exists a variety of approaches. Most of them use gain scheduling to adapt to the vehicle velocity. With the following approach this however not necessary. The control aim is to asymptotically decay the lateral deviation to the reference trajectory

$$\lim_{t\to\infty} \Delta d(t) = 0. \tag{31}$$

For this, the following simplified model is assumed:

$$\begin{bmatrix} \Delta\dot{d} \\ \Delta\dot{\tilde{\theta}} \end{bmatrix} = \begin{bmatrix} 0 & v \\ 0 & 0 \end{bmatrix}\begin{bmatrix} \Delta d \\ \Delta\tilde{\theta} \end{bmatrix} + \begin{bmatrix} 0 \\ -v \end{bmatrix}\kappa_{tc} \tag{32}$$

It results from (5)-(9) with neglecting the vehicle dynamics, the reference curvature and the side slip angle. The reference

curvature is already considered with the feedforward control. The side slip angle is compensated by using an estimator, see (30). This allows to consider the course angle for the feedback law.
The control law for κ_{tc} results directly from the differential equation for Δd (32). By differentiating it until the control input appears, one obtains

$$\Delta\ddot{d} = \dot{v}\Delta\tilde{\theta} + v\Delta\dot{\tilde{\theta}} = \dot{v}\Delta\tilde{\theta} - v^2\kappa_{tc}. \tag{33}$$

It has to satisfy the equation of an ideal damped PT_2 with a desired time constant τ_d:

$$\tau_d^2\Delta\ddot{d} + 2\tau_d\Delta\dot{d} + \Delta d = 0. \tag{34}$$

Solved for the control variable κ_{tc}, results in

$$\kappa_{tc} = \Delta\tilde{\theta}\,\frac{\dot{v}\tau_d^2 + 2v\tau_d}{\tau_d^2 v^2} + \Delta d\,\frac{1}{\tau_d^2 v^2}. \tag{35}$$

This control law ensures the asymptotic decay of lateral deviations. The amplification factors are speed-dependent and thus avoid the need for gain scheduling of the gains. Regardless of the driving speed, the same dynamic behavior of the controlled system results.

Apart from the filter time constants, there remain only the time constant of the nominal vehicle model τ_v and the time constant of the tracking controller τ_d to adjust the controller. The tuning of τ_d and τ_v in order to guarantee robust tracking results is the objective of Section VII.
The feedforward control to calculate the feedforward signal κ_{ff} is implemented as described in [13] and won't be discussed further.

VI. Cooperative Control

As mentioned before, the classical implementation of the DO (see (24)) will not only compensate any disturbances but also the driver input T_h. In spite of this, the modified DO, according to (25), only compensates lateral disturbances, but not the driver's torque. This is possible because the underlying steering angle controller is adapted by the driver's torque (see [6]). According to (23) the control law not only consists of the DO's output κ_{do} but also the tracking controller's output κ_{tc}. The latter is working against the driver input. Similar to impedance and admittance control [14] this control law could also be modified by using the measurement of the driver's torque T_h. However we don't use this because the driver should feel where the driver assistance systems intends to go. The control law of the tracking controller is relatively good-natured compared to the DO's output as the DO has integral behavior. Therefore the output of the tracking controller won't be adapted to the driver input.

VII. Parameter Space Approach

It exists a variety of approaches for selecting the controller parameters τ_d and τ_v. Since significant deviations from the underlying nominal model may occur due to modeling uncertainties or parameter variations (by varying operating conditions such as the varying mass of a vehicle due to different loading) a robust control method is selected, the Parameter Space Approach [15].
Task of the method is to find a controller that meets certain minimum requirements for the control loop, regardless of parameter variations. The desired properties can ask, for example, that the eigenvalues always lie in a given region Γ.

Contrary to the traditional approaches, the parameter space method yields a set of coefficients for a specific controller structure that simultaneously stabilizes a finite number of plants.
For each operating point, the derived Γ stability region will

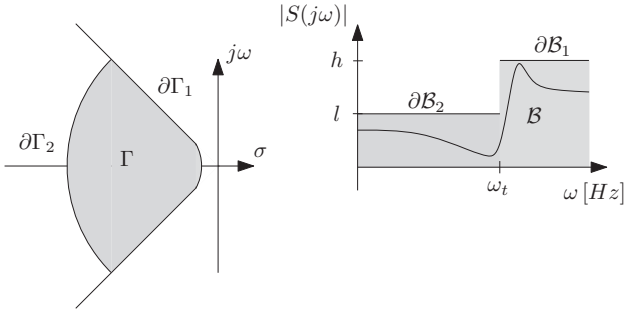

Fig. 6: Example of Γ- and $\mathcal{B}$ regions

be mapped into the controller coefficient space. This will yield to several overlapping Γ stabilizing regions. The system is said to be robustly stable if the operating domain is entirely contained in the intersection of these Γ stabilizing regions.
The region Γ with boundary $\partial\Gamma$ is composed of one or more curves in the s-plane [16]. Fig. 6 shows an example of a Γ stability region.
Γ stability is an approach of meeting the requirements on the system in the time domain solely. To also cover the frequency domain magnitude specifications $\mathcal{B}$ stability can be used. For example it addresses noise and disturbance rejection or robustness against uncertainties in the plant by bounding the magnitude frequency response of specific sensitivity functions [15].
A sensitivity function $S(j\omega)$ is considered to be $\mathcal{B}$ stable if its frequency response magnitude lies within a predefined region $\mathcal{B}$ [15]. By an appropriate selection of $\partial\mathcal{B}(\omega)$ upper bounds can be set to the frequency response magnitude of $S(j\omega)$ so that the preliminary defined requirements regarding the sensitivity of the system to external disturbances can be met:

$$|S(j\omega)| < \partial\mathcal{B}(\omega). \tag{36}$$

$\partial\mathcal{B}(\omega)$ can be derived from the frequency response magnitude specifications on $S(j\omega)$ [15]:

- The maximum steady state error should be limited to l:

$$|S(0)| < l. \tag{37}$$

- The high-frequency disturbance amplification should be limited to h:

$$|S(j\omega)| < h. \tag{38}$$

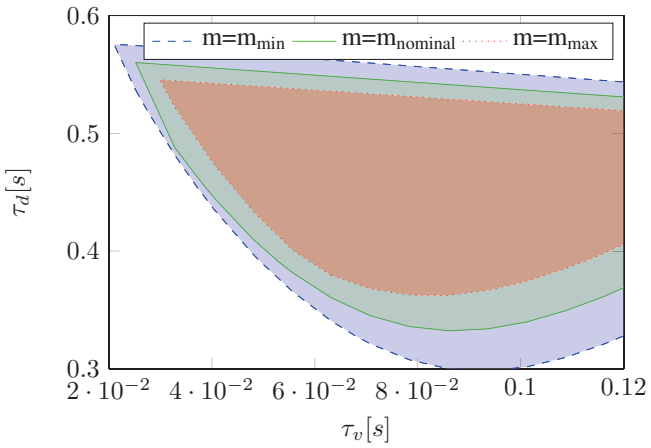

Fig. 7: Γ- and $\mathcal{B}$-stable parameter space for $G_{\kappa_{r,ref}\to\Delta y}(s)$ and $S_{z\dot{\psi}\to\Delta d}(s)$ for different loadings (with v= 50 kph)

- The transition frequency from l to h, i.e. the frequency at which disturbances become amplified instead of attenuated, should be ω_t.

The resulting $\partial\mathcal{B}(\omega)$ (Fig. 6) then becomes:

$$\partial\mathcal{B}(\omega) = \begin{cases} l, & \forall\omega \in [0, \omega_t] \\ h, & \forall\omega \in (\omega_t, \infty) \end{cases} \tag{39}$$

Γ- and $\mathcal{B}-$ specifications are considered for the selection of τ_d and τ_v. The design of the parameters will be shown for a speed of 50 kph by shaping Γ- and $\mathcal{B}$-specification into parameter space of the command step response $G_{\kappa_{r,ref}\to\Delta d}(s)$ and the sensitivity function $S_{z\dot{\psi}\to\Delta d}(s)$ with

$$G_{\kappa_{r,ref}\to\Delta d}(s) = \frac{\Delta d}{\kappa_{r,ref}} \text{ using } \Gamma - \text{Stability} \tag{40}$$

and

$$S_{z\dot{\psi}\to\Delta d}(s) = \frac{\Delta d}{z\dot{\psi}} \text{ using } \mathcal{B} - \text{Stability}. \tag{41}$$

Exemplary the approach is illustrated on a variation of the vehicle mass m. It is varied in a range of

$$m = \begin{cases} m_{min} = m_{nominal} - 250\ kg \\ m_{nominal} \\ m_{max} = m_{nominal} + 250\ kg \end{cases} \tag{42}$$

to select controller parameters stabilizing the vehicle for all permitted loadings. These operations were done by using the "PARADISE"-toolbox which was developed by DLR [17].

Fig. 7 shows the resulting parameter space for different loadings. In this case τ_v and τ_d are selected as $\tau_v = 0.08$ and $\tau_d = 0.5$. The whole procedure can be repeated for different velocities, tire characteristics and different positions of the center of gravity.

VIII. Measurement Results

The control algorithms are implemented in MATLAB/Simulink and run on a dSpace Autobox with a cycle time of 20 ms. As a test vehicle serves a 3 series GT. The trajectory planning calculates trajectories relative to a previously recorded map and the localization is done using a differential GPS platform.

Fig. 8a shows the result of a measurement. The vehicle is driving along a straight reference with a velocity of 50 kph. The driver is intervening and guiding the vehicle 1.2 m to the left. The disturbance observer's output κ_{do} is almost all the time 0 as there is no disturbance acting on the vehicle besides the driver. The tracking controller however is working moderately against the driver, guiding the vehicle back to the reference after the driver's torque is zero again.

Fig. 8b shows a second maneuver, representing the suppression of side-force disturbances. Again the vehicle has to follow a straight line with 50 kph. A side-force disturbance is generated by one-sided braking. Therefore the vehicle's right front and rear wheels are both exposed to 500 Nm braking torque. This leads to a side-force disturbance. The disturbance observer rejects this disturbance with minimal control error.

IX. Conclusion and Future Works

Future driver assistance systems will support the driver by partly or fully taking over the lateral control. This paper therefore presented a structure for handling both autonomous as well as cooperative maneuvers with driver interaction. In both cases lateral force disturbances are robustly compensated. This is achieved by modifying the usual disturbance observer structure to only compensate a certain part of the disturbances (the lateral force disturbances) with treating the driver's torque not as a disturbance.

Appendix A
Single-Track Model

For the design of the controller the single-track model was used resulting the transfer functions $G_{\dot{\psi}}(s)$ and $G_{\beta}(s)$. The equations of the single-track model [5] results from equilibrium of forces in lateral direction (see Fig. 9)

$$m(\dot{\beta}v_x + \dot{\psi}v_x) = c_f\alpha_f + c_r\alpha_r \tag{43}$$

and the moment equilibrium

$$J\ddot{\psi} = c_f\alpha_f l_f - c_r\alpha_r l_r. \tag{44}$$

m describes the vehicle mass and J the moment of inertia with respect to the yaw axis at the center of gravity (COG). The distances between the COG and the front and rear axle are referred as l_f and l_r. The wheelbase results as $l = l_r + l_f$. The angle between the wheel's longitudinal axis and the wheel's velocity is defined as the slip angle α. The slip angle of the front axis α_f calculates as

$$\alpha_f = \delta - \beta - l_f\frac{\dot{\psi}}{v} \tag{45}$$

and the rear slip angle α_r as

$$\alpha_r = -\beta + l_r\frac{\dot{\psi}}{v}. \tag{46}$$

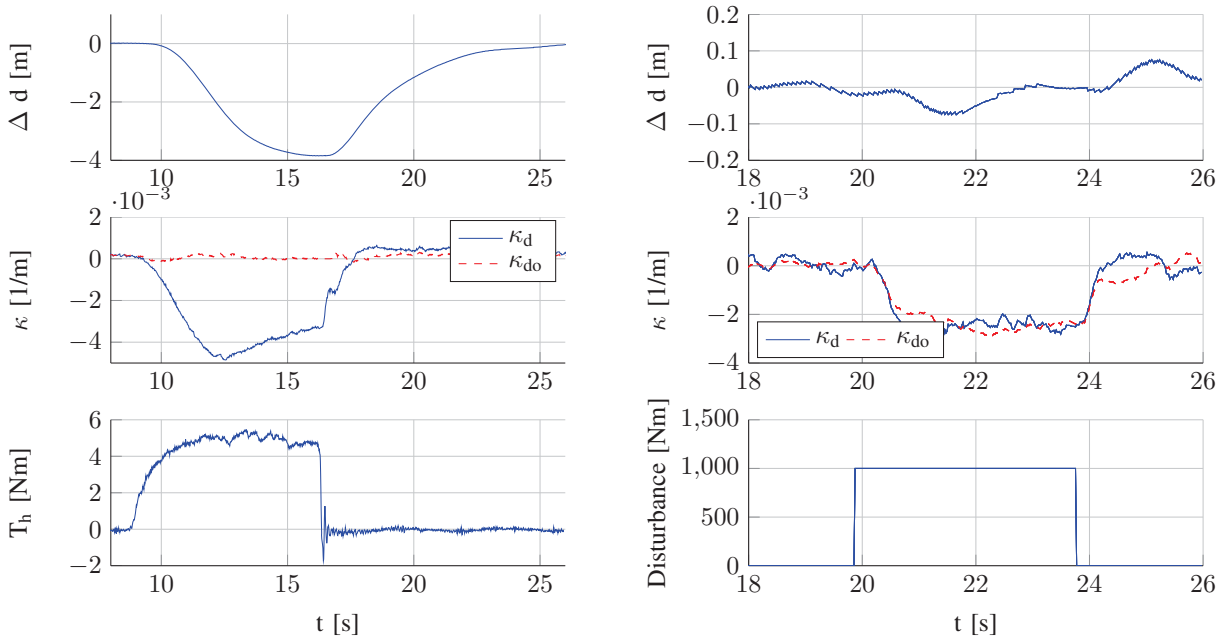

(a) Driver intervention

(b) Side-force rejection

Fig. 8: Measurement results

By introducing the tire's relaxation length σ the transient tire characteristic is taken into account. Applied to the front axle results

$$\frac{\sigma_f}{v}\dot{F}_{sf} + F_{sf} = c_f \alpha_f \tag{47}$$

and for the rear tires

$$\frac{\sigma_r}{v}\dot{F}_{sr} + F_{sf} = c_r \alpha_r. \tag{48}$$

The relaxation length of the tire depends on the vehicle speed and tire condition. The cornering stiffness of the wheel are denoted as c_f and c_r. Combining (43)-(48) and writing it in state-space representation results in

$$\begin{bmatrix} \ddot{\psi} \\ \dot{\beta} \\ \dot{F}_{sf} \\ \dot{F}_{sr} \end{bmatrix} = \begin{bmatrix} 0 & 0 & \frac{l_f}{J_{fzg}} & -\frac{l_r}{J_{fzg}} \\ -1 & 0 & \frac{1}{mv} & \frac{1}{mv} \\ -\frac{c_f}{\sigma_f} l_f & -v\frac{c_f}{\sigma_f} & -\frac{v}{\sigma_f} & 0 \\ \frac{c_r}{\sigma_r} l_r & -v\frac{c_r}{\sigma_r} & 0 & -\frac{v}{\sigma_r} \end{bmatrix} \begin{bmatrix} \dot{\psi} \\ \beta \\ F_{sf} \\ F_{sr} \end{bmatrix} + \begin{bmatrix} 0 \\ 0 \\ v\frac{c_f}{\sigma_f} \\ 0 \end{bmatrix} \delta. \tag{49}$$

This can be solved for the required transfer functions $G_{\dot{\psi}}(s)$ and $G_{\beta}(s)$.

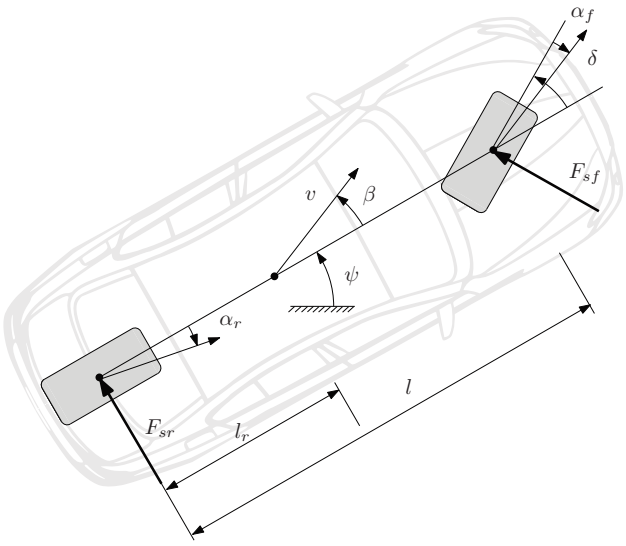

Fig. 9: Single-track model

References

[1] K. Ohnishi, "A new servo method in mechatronics," *Trans. Jpn. Soc. Elect. Eng*, vol. 107, pp. 83–86, 1987.

[2] J. Ackermann, J. Guldner, W. Sienel, R. Steinhauser, and V. I. Utkin, "Linear and nonlinear controller design for robust automatic steering," *Control Systems Technology, IEEE Transactions on*, vol. 3, no. 1, pp. 132–143, 1995.

[3] M. Werling, L. Gröll, and G. Bretthauer, "Invariant trajectory tracking with a full-size autonomous road vehicle," *IEEE Transactions on Robotics*, vol. 26, no. 4, pp. 758–765, 2010.

[4] R. Attia, R. Orjuela, and M. Basset, "Coupled longitudinal and lateral control strategy improving lateral stability for autonomous vehicle," in *American Control Conference (ACC), 2012*. IEEE, 2012, pp. 6509–6514.

[5] P. Riekert and T.-E. Schunck, "Zur Fahrmechanik des gummibereiften Kraftfahrzeugs," *Ingenieur-Archiv*, vol. 11, no. 3, pp. 210–224, 1940.

[6] M. Walter, N. Nitzsche, D. Odenthal, and S. Müller, "Lateral vehicle guidance control for autonomous and cooperative driving," in *Proc. European Control Conference*. European Control Conference, 2014, pp. 2667–2672.

[7] B. A. Güvenç, L. Güvenç, and S. Karaman, "Robust MIMO disturbance observer analysis and design with application to active car steering," *International Journal of Robust and Nonlinear Control*, vol. 20, no. 8, pp. 873–891, 2010.

[8] T. Umeno and Y. Hori, "Robust speed control of DC servomotors using modern two degrees-of-freedom controller design," *Industrial Electronics, IEEE Transactions on*, vol. 38, no. 5, pp. 363–368, 1991.

[9] S.-K. Park and S.-H. Lee, "Disturbance observer based robust control for industrial robots with flexible joints," in *Control, Automation and Systems, 2007. ICCAS'07. International Conference on*. IEEE, 2007, pp. 584–589.
[10] S. M. Shahruz, "Suppression of effects of nonlinearities by disturbance observers," in *American Control Conference, 2004. Proceedings of the 2004*, vol. 5. IEEE, 2004, pp. 4342–4347.
[11] H. Shim and N. H. Jo, "An almost necessary and sufficient condition for robust stability of closed-loop systems with disturbance observer," *Automatica*, vol. 45, no. 1, pp. 296–299, 2009.
[12] B. A. Guvenc, T. Bunte, D. Odenthal, and L. Guvenc, "Robust two degree-of-freedom vehicle steering controller design," *Control Systems Technology, IEEE Transactions on*, vol. 12, no. 4, pp. 627–636, 2004.
[13] C. Rathgeber, F. Winkler, D. Odenthal, and S. Müller, "Lateral trajectory tracking control for autonomous vehicles," in *Proc. European Control Conference*. European Control Conference, 2014, pp. 1024–1029.
[14] N. Hogan, "Impedance control: An approach to manipulation," in *American Control Conference, 1984*. IEEE, 1984, pp. 304–313.
[15] J. Ackermann and P. Blue, *Robust control: the parameter space approach*. Springer, 2002.
[16] J. Ackermann, A. Bartlett, D. Kaesbauer, W. Sienel, and R. Steinhauser, *Robust control*. Springer, 1993.
[17] W. Sienel, T. Bunte, and J. Ackermann, "Paradise-parametric robust analysis and design interactive software environment: A matlab-based robust control toolbox," in *Computer-Aided Control System Design, 1996., Proceedings of the 1996 IEEE International Symposium on*. IEEE, 1996, pp. 380–385.